

A Different Extensional Viscosity Prediction Based on Entry Pressure Drop

Jia Yang,^{1,2} Yahui Dai,¹ Jigong Li¹

¹School of Material Science and Engineering, Henan Polytechnic University, Jiaozuo 454000 People's Republic of China

²Cultivating Base for Key Laboratory of Environment-Friendly Inorganic Materials in University of Henan Province, Henan Polytechnic University, Jiaozuo 454000 People's Republic of China

Correspondence to: J. Yang (E-mail: jiangshanjia@163.com)

ABSTRACT: Extensional viscosity, an important processing parameter, can control the processing properties of polymeric products in industrial processes, such as fiber spinning, blow molding, and film casting. In this article, based on the equivalent thought, the contraction flow in the circular channel was studied without using the power laws, and the new equations of the extensional strain rate and the extensional viscosity based on entry pressure drop were proposed. The extensional viscosity of two high-density polyethylene melts was predicted using the proposed equations, the Cogswell's equations, the Binding's equations, and the Gibson's equations. Moreover, this prediction was compared with the experimental data of the extensional viscosity. It was found that the predicted extensional viscosity of the proposed equations was close to the experimental data. © 2014 Wiley Periodicals, Inc. *J. Appl. Polym. Sci.* **2014**, *131*, 40563.

KEYWORDS: entry contraction flow; entry pressure drop; extensional viscosity; prediction; shear flow

Received 25 October 2013; accepted 4 February 2014

DOI: 10.1002/app.40563

INTRODUCTION

Extensional flow is a common flow in industrial processes, such as fiber spinning, blow moulding, and film casting. Extensional viscosity, an important processing parameter of the extensional flow, can influence the processing properties of the polymeric products.^{1–5} Studying the extensional viscosity under different conditions can be helpful to reveal the flow mechanisms, and provide some guidelines for optimizing processing technology. Many extensional rheometers have been made to measure the extensional viscosity of the polymer fluids. Nevertheless, these devices remain time-consuming and it is difficult to obtain the extensional viscosity in the wide range of the extensional strain rates.^{2,3,6–11}

When the polymer fluid flows from the extruder barrel to the die in the polymer process, the entry contraction flow appears subjected to the deformation of the shear and the extension, and the entry pressure drop occurs accordingly.^{2,12–14} Compared with the measurement of the extensional viscosity, the measurements of the entry pressure drop and the shear viscosity are easy to perform.^{2,15} An economical and effective approach to obtain the extensional viscosity is based on the experimental data of the entry pressure drop and the shear viscosity.² This approach has been studied extensively since 1970s.^{2,12–14} According to the force balance, Cogswell¹² proposed a simple method to determine the extensional viscosity based on the force balance, but the prediction of the extensional viscosity

deviated from the experimental data for some polymer melts.^{9,16–18} Binding¹³ made an approximate analysis for the contraction flow using power laws of the shear viscosity and the extensional viscosity to predict the extensional flow. Some researchers^{16,19,20} considered that the strain rate along the flow direction was zero at the edge of the contraction region, whereas the rate was not zero in the Binding's derivations.¹³

The equivalent thought, used to solve many complex problems of the mechanics, the electric conduction, and the heat conduction,^{21–23} makes the complicated problems simplified by proposing simple schemes or ideas. Previously, the authors²¹ combined the equivalent volume of the carbon black aggregate into the general effective media theory, and the predicted results of the electrical conductivity and the percolation threshold were in agreement with experimental data.

The power laws of the shear viscosity and the extensional viscosity are not suitable at low deformational rates, and the extensional strain rate in the contraction flow is complex for the polymer fluids.^{16,19,20} The purpose of this article is to study the abrupt contraction flow in the circular channel without using the power laws, and analyze the extensional strain rate based on the equivalent thought, so as to propose new equations of the extensional strain rate and extensional viscosity. The predicted extensional viscosity based on the proposed equations was compared with the measured extensional viscosity. In final, the predictive ability of different equations is discussed.

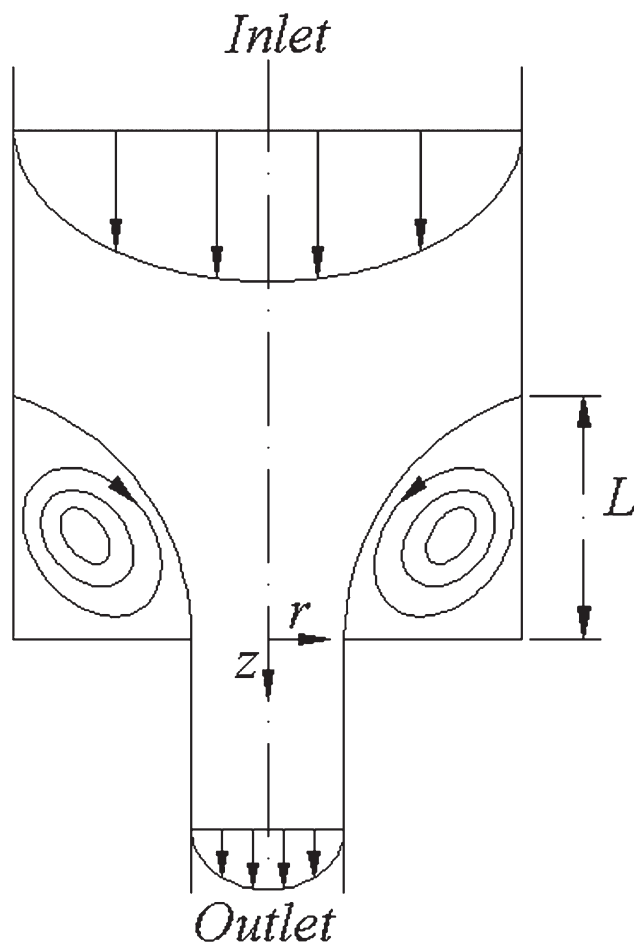


Figure 1. Sketch of the abrupt contraction flow of the polymer fluid in the circular channel.

THEORETICAL ANALYSIS

Basic Hypotheses and Equations

The basic hypotheses of the theoretical analysis are as follows: (1) the polymer fluid is isothermal and incompressible; (2) the polymer fluid can not slip in the pipe wall; (3) the inertial and the weight of the polymer fluid are ignored. Figure 1 is the sketch of the abrupt contraction flow of the polymer fluid in the circular channel. The cylindrical polar coordinates (r , θ , z) are used. The polymer fluid flows along the z -axis which is perpendicular to r -axis, and the axis of symmetry in the contraction flow is $y = 0$. The polymer fluid flows in the large circular channel (its radius is R_1) ($z \leq 0$), and suddenly enters at $z = 0$ into the small circular channel (its radius is R_0). Thus, the velocities in the z -axis and the r -axis can be written as, respectively.¹³

$$v_z = \frac{Q(1+3n)}{\pi R^2(1+n)} \left[1 - \left(\frac{r}{R} \right)^{\frac{1+n}{n}} \right] \quad (1)$$

$$v_r = \frac{rQ(1+3n)}{\pi R^3(1+n)} \left[1 - \left(\frac{r}{R} \right)^{\frac{1+n}{n}} \right] \frac{dR}{dz} \quad (2)$$

where n is the non-Newtonian index, Q is the volumetric flow rate, R is the distance from the center line to the vortex, and is the function of z .

In the abrupt contraction flow of the polymer fluid, $\frac{dR}{dz}$ is small, the terms involving $\left(\frac{dR}{dz}\right)^2$ and $\frac{d^2R}{dz^2}$ can be neglected.¹³ The shear rate at the radius r , deduced from eqs. (1) and (2), can be written as:¹³

$$\dot{\gamma}_r = \frac{\partial v_z}{\partial r} + \frac{\partial v_r}{\partial z} = -\frac{Q(1+3n)}{\pi n R^3} \left(\frac{r}{R} \right)^{\frac{1}{n}} \quad (3)$$

and the extensional strain rate at the radius r , deduced from eq. (1), can be written as:¹³

$$\dot{\epsilon}_r = \frac{\partial v_z}{\partial z} = -\frac{2v_z}{R} \frac{dR}{dz} + \frac{Q(1+3n)}{\pi R^3(1+n)} \left[\frac{1+n}{n} \left(\frac{r}{R} \right)^{\frac{1+n}{n}} \right] \frac{dR}{dz} \quad (4)$$

Analysis

In general, the extensional strain rate is zero at the edge of the contraction region,^{16,19,20} whereas the rate is not zero in eq. (4). Previously, Mackay and Astarita¹⁶ neglected the last item of eq. (4) to make the extensional strain rate be zero. Here, the equivalent extensional strain rate replaces the extensional strain rate. To keep the conservation of the extensional deformation, the total extensional strain rate in the contraction flow can be written as

$$\dot{\epsilon}_{\text{tot}} = \int_0^R 2\pi r |\dot{\epsilon}_r| dr = \int_0^R 2\pi r \dot{\epsilon}_{re} dr \quad (5)$$

where $\dot{\epsilon}_{re}$ is the equivalent extensional strain rate at the radius r . Based on the equivalent thought, the equivalent extensional strain rate at the radius r , deduced from eq. (5), can be written as:

$$\dot{\epsilon}_{re} = \frac{N v_z}{R} \frac{dR}{dz} \quad (6)$$

where N is the function of the flow behavior index, and can be written as:

$$N = \frac{8n}{1+n} \left[\left(\frac{2n}{1+3n} \right)^{\frac{n-1}{1+n}} - \left(\frac{2n}{1+3n} \right)^{\frac{2n}{1+n}} \right] \quad (7)$$

According to the previous analysis,^{13,16,24} the total power can be written as:

$$W = \int (W_s + W_e) 2\pi r dr dz \quad (8)$$

where W_s is the shear dissipation per unit volume, W_e is the extensional dissipation per unit volume. Because the power laws of the shear viscosity and the extensional viscosity are not suitable at low deformational rates,²⁰ W_s and W_e are written as, respectively.

$$W_s = \dot{\gamma}_r \tau_{rz} = \eta_s \dot{\gamma}_r^2 \quad (9)$$

$$W_e = \dot{\epsilon}_r (\tau_{zz} - \tau_{rr}) = \eta_e \dot{\epsilon}_{re}^2 \quad (10)$$

where η_s is the shear viscosity defined as the ratio of the shear stress to the shear rate and η_e is the extensional viscosity defined as the ratio of the extensional stress to the extensional strain rate. Substituting eqs. (1), (3), (6), and (7), (9) and (10) into eq. (8), the total power in the contraction region can be written as

Table I. The Molecular Characteristics of Two HDPE⁹

HDPE	M_w (g/mol)	M_n (g/mol)	M_w/M_n
A	208,000	14,000	14.9
B	150,000	16,000	9.4

Where M_n is number average molecular mass, M_w is weight average molecular mass, M_w/M_n is polydispersity coefficient.

$$W = \int_{-L}^0 \left\{ \frac{\pi \eta_s R^2}{1+n} \left[\frac{Q(1+3n)}{\pi R^3} \right]^2 + \frac{\pi \eta_e R^2 N^2}{(1+2n)(1+3n)} \left[\frac{Q(1+3n)}{\pi R^3} \right]^2 \left(\frac{dR}{dz} \right)^2 \right\} dz$$

$$= \int_{-L}^0 f \left(R, \frac{dR}{dz} \right) dz \quad (11)$$

where L is the vortex length on z -axis, and f is the function of R and $\frac{dR}{dz}$. The flow of the polymer melt in the contraction region accords to the minimum energy dissipated. Thus, using the Euler's equation of the variational calculus,²⁵ the following expression can be deduced from eq. (11).

$$\frac{dR}{dz} = \frac{1}{N} \left[\frac{\eta_s(1+2n)(1+3n)}{\eta_e(1+n)} \right]^{\frac{1}{2}} \quad (12)$$

Substituting eq. (12) into eq. (11), the entry pressure drop can be written as:

$$\Delta P_{\text{ent}} = \frac{W}{Q} = \frac{2N\dot{\gamma}(1+3n)(1-\alpha^{-3})}{3(1+n)} \left[\frac{\eta_s \eta_e n(1+n)}{(1+2n)(1+3n)} \right]^{\frac{1}{2}} \quad (13)$$

where $\dot{\gamma}$ is the shear rate in the small circular channel given by $\frac{Q(1+3n)}{\pi R_0^3}$, and α is the contraction ratio given by $\frac{R_0}{R}$. Substituting eqs. (7) and (13) into the eq. (6) with the method of the calculus,²⁵ the average extensional strain rate at the orifice is written as:

$$\dot{\epsilon} = \frac{2N\eta_s \dot{\gamma}^2 (1-\alpha^{-3})}{3\Delta P_{\text{ent}} (1+n)} \quad (14)$$

The extensional viscosity derived from eq. (13) can be written as:

$$\eta_e = \frac{9\Delta P_{\text{ent}}^2 (1+n)(1+2n)}{4\eta_s n N^2 \dot{\gamma}^2 (1+3n)(1-\alpha^{-3})^2} \quad (15)$$

EXPERIMENTAL

Baldi et al.⁹ conducted the rheology of the two high-density polyethylene (HDPE), supplied by Polimeri Europa SpA in Italy at 180°C. The two HDPE melts are labeled as A and B, and their molecular characteristics are reported in Table I.⁹ The shear viscosity and the entry pressure drop were measured by a capillary rheometer Rheologic 5000 by Ceast SpA in Italy. The diameter was 0.001 m and the length-diameter ratios were 10, 20, and 30 for the circular capillary. The contraction ratio was 15. The entry pressure drop was determined with the Bagley's plot method.

The extensional viscosity of two HDPE melts was obtained from a tensile test and a melt spinning test. In the tensile test,

the polymer sample of narrow long rod was prepared via extrusion through a circular die with a diameter of 0.002 m. Before the tensile test was performed, the sample was left for several minutes in the oil bath at 180°C to allow the sample to relax the macromolecular preorientation induced under extrusion, and the dependence of the extensional viscosity on the extensional strain rate was obtained at the extensional strain rate of 0.01, 0.1, and 0.5 s⁻¹. The extensional viscosity was obtained from the melt spinning experiment at high extensional strain rates. In such test, the polymer filament, extruded at a constant extrusion rate through a circular die (The diameter was 0.001 m and the length-diameter ratio was 30), was drawn by the pinching rotating wheels and the extensional force was measured until the sample breakage. The extensional acceleration speed was 0.005 m/s², and the spinline length was 0.2 m. The dependence of the extensional viscosity on the extensional strain rate was obtained based on the Newtonian local approach. For detailed descriptions of the experiment, see Baldi et al.⁹ Figure 2 shows that the apparent shear viscosity and the entry pressure drop at different apparent shear rates for material A.⁹ Figure 3 shows that the apparent shear viscosity and the entry pressure drop at different apparent shear rates for material B.⁹

EXPERIMENTAL VERIFICATION AND COMPARISON

As stated above, it is difficult to obtain true steady extensional viscosity,^{2,3,6-11} the common technique for measuring extensional viscosity of polymer melts are the tensile test and the melt spinning test, so the experimental data of Baldi et al.⁹ are adopted to examine predictive ability of the proposed equations objectively. Based on the experimental data of entry pressure drop and apparent shear viscosity in Figures 2 and 3, the predicted extensional viscosity calculated from the proposed eqs. (14) and (15) is compared with the experimental data of two HDPE melts. Figures 4 and 5 show the comparison between experimental data and prediction for materials A and B, respectively. It can be found from Figures 4 and 5 that the extensional viscosity decreases with the extensional strain rate increasing, and the experimental data from the melt spinning test disagree with those from the tensile test, the former are overestimated with respect to the latter at low extensional strain rates ($\dot{\epsilon} \leq 4\text{s}^{-1}$ for material A, $\dot{\epsilon} \leq 10\text{s}^{-1}$ for material B). This

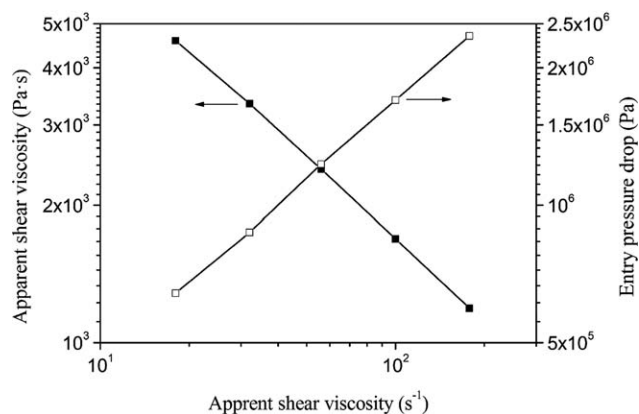


Figure 2. Apparent shear viscosity and entry pressure drop at different apparent shear rates for material A.⁹

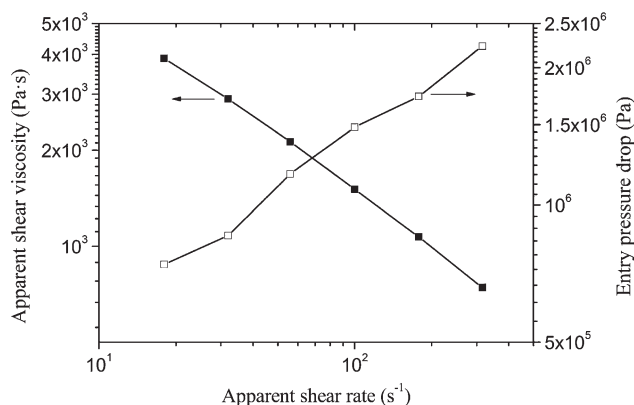


Figure 3. Apparent shear viscosity and entry pressure drop at different apparent shear rates for material B.⁹

discrepancy at low extensional strain rates for the melt spinning test could be explained by the fact that the strain contribution of the entry region and the shear region during the extrusion process results in the additional macromolecular preorientation which hinders the extensional flow.⁹ Conversely, because of relatively low temperature in the melt spinning environment, the polymer melt was cooled slightly under stretching, and the extensional resistance increases.³ Thus, the extensional resistance induced by the macromolecular preorientation and the cooling cannot be ignored with respect to the small extensional force at low extensional strain rates, and the extensional viscosity increases accordingly. With the extensional strain rate increasing, the extensional force increases, the cooling time shortens, and the cooling degree decreases in the extensional region. The extensional resistance induced can be ignored with respect to the large extensional force at high extensional strain rates.

This discrepancy also indicates that the extensional force in the melt spinning test is measured under quasiisothermal and quasi-steady conditions,^{9,11} especially at low extensional strain rates. While the melt spinning test is widely adopted owing to its experimental simplicity and closed industrial polymer processes, such as fiber spinning and film blowing.^{3,9,26–28} It can be also found from Figures 4 and 5 that the prediction of eqs. (14) and (15) based on the entry pressure drop and the shear viscosity are in good agreement with the experimental data of the extensional viscosity for two HDPE melts, although slightly underestimated with respect to the experimental data at low extensional strain rates for the melt spinning test.

Previously, Cogswell¹² proposed the equations of the extensional strain rate and the extensional viscosity, and the extensional strain rate and the extensional viscosity can be written as, respectively

$$\dot{\epsilon} = \frac{4\eta_a \dot{\gamma}_a^2}{3\Delta P_{\text{ent}}(1+n)} \quad (16)$$

$$\eta_e = \frac{9\Delta P_{\text{ent}}^2(1+n)^2}{32\eta_a \dot{\gamma}_a^2} \quad (17)$$

where η_a is the apparent shear viscosity in the small circular channel given by $\frac{\eta_a(1+3n)}{4n}$, and $\dot{\gamma}_a$ is the apparent shear rate in the small circular channel given by $\frac{4Q}{\pi R_0^2}$. Based on the Binding's

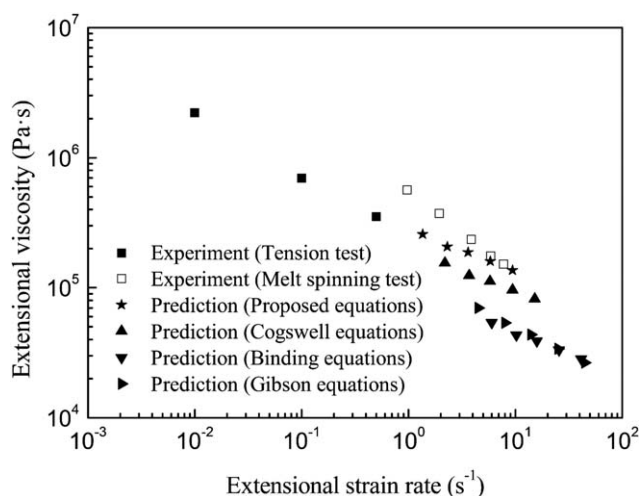


Figure 4. Comparison between experimental data and prediction of the proposed equations, the Cogswell's equations, the Binding's equations, and Gibson's equations for material A.

analysis,¹³ the extensional strain rate and the extensional viscosity can be written as follows:

$$\dot{\epsilon} = \frac{\eta_a \dot{\gamma}_a^2 (1+3n)(1+k)^2}{3\Delta P_{\text{ent}} k^2 (1+n)^2} \left(\frac{1+3n}{4n} \right)^n \quad (18)$$

$$\eta_e = \frac{9\Delta P_{\text{ent}}^2 k^3 2^{k-1} (1+n)^4}{I \eta_a \dot{\gamma}_a^2 (1+3n)^2 (1+k)^4} \left(\frac{4n}{1+3n} \right)^n \quad (19)$$

where I is an integral defined as:

$$I = \int_0^1 \left\{ \text{abs} \left[2 - \left(\frac{1+3n}{n} \right) \zeta^{\frac{1+n}{n}} \right] \right\}^{1+k} \zeta d\zeta \quad (20)$$

k can be written as $\frac{t}{1+n}$ and t is the slope of a log-log plot of ΔP_{ent} versus $\dot{\gamma}_a$. Gibson²⁹ assumed power law behavior for the

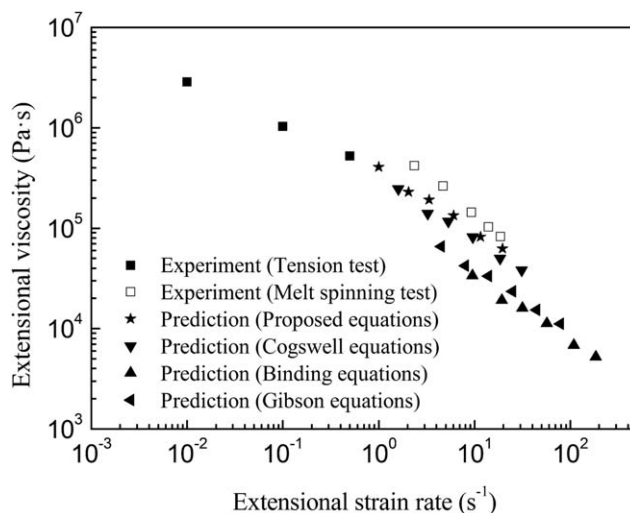


Figure 5. Comparison between experimental data and prediction of the proposed equations, the Cogswell's equations, the Binding's equations, and Gibson's equations for material B.

shear and extensional viscosities and obtained the following expressions as follows:

$$\dot{\epsilon} = \frac{\dot{\gamma}_a}{4} \quad (21)$$

$$\eta_e = \frac{12g\Delta P'_{ent}}{2\dot{\gamma}_a(1-\alpha^{-3g}) + 3gH\dot{\gamma}_a} \quad (22)$$

where H and $\Delta P'_{ent}$ is can be written as, respectively

$$H = \int_0^{\frac{\pi}{2}} (1 + \cos \beta)^{g-1} (\sin \beta)^{1+g} d\beta \quad (23)$$

$$\Delta P'_{ent} = \Delta P_{ent} - \frac{2^{2+3n}\eta_a\dot{\gamma}_a}{3n\pi^{1+3n}} \left(\frac{1+3n}{4n}\right)^n (1-\alpha^{-3n}) \quad (24)$$

The parameter g is the slope of a log-log plot of $\Delta P'_{ent}$ versus $\dot{\gamma}_a$.

As shown in Figures 4 and 5, the predictive capability of the proposed equations, the Cogswell's equations, the Binding's equations, and the Gibson's equations is compared. It can be found that the prediction of eqs. (14) and (15) are larger than those of the Cogswell's equations, the Binding's equations, and the Gibson's equations. Furthermore, the proposed equations based on the entry pressure drop can well predict the extensional viscosity of two HDPE melts at high extensional strain rates as shown in Figures 4 and 5. Generally, it is difficult to obtain the experimental data of the extensional viscosity, especially at high extensional strain rates.^{2,3,7-10} The experimental verification and model comparison above indicate that it is a simple method to predict the extensional viscosity using the proposed equations, which is helpful to control and monitor the polymer processing.

CONCLUSIONS

In this article, the extensional strain rate was proposed based on the equivalent thought in the abrupt contraction flow of the circular channel, the contraction flow was studied based on the minimum energy without using the power laws, and the new equations of the extensional strain rate and the extensional viscosity based on the entry pressure drop were derived. The predicted extensional viscosity of the proposed equations was larger than those of the Cogswell's equations, the Binding's equations, and the Gibson's equations and was close to the experimental data of two HDPE melts.

ACKNOWLEDGMENTS

This work was supported by the Science and Technology Research Project of Education Department of Henan Province (No. 14B430013) and the Doctoral Fund Project of Henan Polytechnic University (No. B2013-016).

REFERENCES

- Zatloukal, M.; Vlček, J.; Tzoganakis, C.; Sába, P. *J. Nonnewton. Fluid Mech.* **2002**, *107*, 13.

- Zatloukal, M.; Musil, J. *Polym. Test.* **2009**, *28*, 843.
- Yang, J.; Liang, J. Z.; Li, F. J. *J. Macromol. Sci., Phys.* **2012**, *51*, 1715.
- Liang, J. Z.; Zhong, L.; Wang, K. J. *J. Appl. Polym. Sci.* **2012**, *125*, 2202.
- Liang, J. Z.; Zhong, L. *Colloid. Polym. Sci.* **2013**, *291*, 1595.
- Meissner, J.; Hostettler, J. *Rheol. Acta* **1994**, *33*, 1.
- Sentmanat, M.; Wang, B. N.; McKinley, G. H. *J. Rheol.* **2005**, *49*, 585.
- Aho, J.; Rolón Garrido, V. H.; Syrjälä, S.; Wagner, M. H. *Rheol. Acta* **2010**, *49*, 359.
- Baldi, F.; Franceschini, A.; Riccò, T. *Rheol. Acta* **2007**, *46*, 965.
- Handge, U. A.; Schmidheiny, W. *Rheol. Acta* **2007**, *46*, 913.
- Petrie, C. J. *J. Nonnewton. Fluid Mech.* **2006**, *137*, 15.
- Cogswell, F. N. *Polym. Eng. Sci.* **1972**, *12*, 64.
- Binding, D. M. *J. Nonnewton. Fluid Mech.* **1988**, *27*, 173.
- Liang, J. Z. *Polym. Plast. Technol. Eng.* **2007**, *46*, 475.
- Liang, J. Z.; Yang, J.; Tang, C. Y. *J. Appl. Polym. Sci.* **2011**, *119*, 1835.
- Mackay, M. E.; Astarita, G. *J. Nonnewton. Fluid Mech.* **1997**, *70*, 219.
- Aho, J.; Rolón Garrido, V. H.; Syrjälä, S.; Wagner, M. H. *J. Nonnewton. Fluid Mech.* **2010**, *165*, 212.
- Padmanabhan, M.; Macosko, C. W. *Rheol. Acta* **1997**, *36*, 144.
- Leonov, A. I. *Polym. Int.* **1995**, *36*, 187.
- Han, C. D. *Rheology and Processing of Polymeric Materials: Polymer Processing*; Oxford University Press: New York, **2007**.
- Yang, J.; Liang, J. Z. *Polym. Int.* **2011**, *60*, 738.
- Marcos-Gómez, D.; Ching-Lloyd, J.; Elizalde, M. R.; Clegg, W. J.; Molina-Aldareguia, J. M. *Compos. Sci. Technol.* **2010**, *70*, 2276.
- Brune, D. A.; Bicerano, J. *Polymer* **2002**, *43*, 369.
- Lubansky, A. S.; Boger, D. V.; Servais, C.; Burbidge, A. S.; Cooper-White, J. J. *J. Nonnewton. Fluid Mech.* **2007**, *144*, 87.
- Fomin, S. V.; Silverman, R. A. *Calculus of Variations*; Dover: New York, **2000**.
- Wagner, M. H.; Collignon, B.; Verbeke, J. *Rheol. Acta* **1996**, *35*, 117.
- Wagner, M. H.; Bernnat, A.; Schulze, V. *J. Rheol.* **1998**, *42*, 917.
- Muke, S.; Ivanov, I.; Kao, N.; Bhattacharya, S. N. *J. Nonnewton. Fluid Mech.* **2001**, *101*, 77.
- Gibson, A. In *Rheological Measurement*; Collyer, A., Clegg, D., Eds.; Chapman and Hall: London, **1998**.